Journal of Molecular Structure 1125 (2016) 350–357

Contents lists available at ScienceDirect

Journal of Molecular Structure

journal homepage: http://www.elsevier.com/locate/molstruc

First-principles study of the structural, elastic, vibrational, thermodynamic and electronic properties of the Mo_2B intermetallic under pressure

R. Escamilla [a, *], E. Carvajal [b], M. Cruz-Irisson [b], M. Romero [c], R. Gómez [c], V. Marquina [c], D.H. Galván [d], A. Durán [d]

[a] Instituto de Investigaciones en Materiales, Universidad Nacional Autónoma de México, Apartado Postal 70-360, México D.F., 04510, Mexico
[b] ESIME-Culhuacán, Instituto Politécnico Nacional, Av. Santa Ana 1000, C.P. 04430, México, D.F., Mexico
[c] Facultad de Ciencias, Universidad Nacional Autónoma de México, Apartado Postal 70-399, México D.F., 04510, Mexico
[d] Centro de Nanociencias y Nanotecnología, Universidad Nacional Autónoma de México, Km. 107 Carretera Tijuana-Ensenada, Apartado Postal 14, C.P. 22800, Ensenada, BC, Mexico

ARTICLE INFO

Article history:
Received 12 January 2016
Received in revised form
30 June 2016
Accepted 1 July 2016
Available online 5 July 2016

Keywords:
Dimolybdenum boride
Phonons
Electron density of states
High pressure

ABSTRACT

The structural, elastic, vibrational, thermodynamic and electronic properties of the Mo_2B intermetallic under pressure are assessed using first-principles calculations based on the generalized gradient approximation (GGA) proposed by Perdew-Wang (PW91). Our results show that the calculated structural parameters at a pressure of zero GPa are in good agreement with the available experimental data. The effect of high pressures on the lattice constants shows that the compression along the c-axis and along the a-axis are similar. The elastic constants were calculated using the static finite strain technique, and the bulk shear moduli are derived from the ideal polycrystalline aggregate. We find that the elastic constants, elastic modulus and hardness monotonically increase as a function of pressure; consequently, the structure is dynamically stable and tends from brittle to ductile behavior under pressure. The Debye temperature θ_D increases and the so-called Grüneisen constant γ decreases due to stiffening of the crystal structure. The phonon dispersion curves were obtained using the direct method. Additionally, the internal energy (ΔE), the Helmholtz free energy (ΔF), the entropy (S) and the lattice contribution to the heat capacity C_v were calculated and analyzed with the help of the phonon dispersion curves. The $N(E_F)$ and the electron transfer between the B and Mo atoms increase as a function of pressure.

1. Introduction

Transition-metal borides have been attracting considerable attention due to their interesting physical properties, such as high melting point, high hardness, low compressibility, thermal stability, excellent electric conductivity and good mechanical properties [1–7].

The total solubility of B in the Mo matrix gives rise to a few interesting intermetallic phases that have been studied extensively from experimental and theoretical perspectives. In the Mo–B phase diagram, there are six known phases, as shown in Fig. 1(a) [8]. These phases are α-MoB (tetragonal structure, low-temperature space group $I4_1/amd$, Z = 8) [1], β-MoB (orthorhombic structure, high-temperature space group $Cmcm$, Z = 4) [2], Mo_2B (tetragonal structure, space group $I4/mcm$, Z = 4) [1], MoB_2 (hexagonal structure, space group $P6/mmm$, Z = 1) [2,3], Mo_2B_5 (rhombohedral structure, space group R-3m, Z = 6) [1] and MoB_4 (hexagonal structure, space group $P6_3/mmc$, Z = 4) [4].

These phases exhibit interesting mechanical and electronic properties. The brittle nature, hardness and high wear resistance in some phases rich in B are attractive for engineering applications. For example, the brittle nature increases with increasing B/Mo ratio, i.e., Mo_2B is less brittle than MoB_4 [9]. From a basic perspective, some of these phases surprisingly exhibit superconductivity, such as MoB ($T_c = 0.5$ K [6]) and Mo_2B ($T_c = 5.86$ K [7]). Investigations of the electronic properties of the Mo-B phases have shown that the major contribution to the electronic density of states at the Fermi level is the Mo 4d states, which are the main states responsible for

* Corresponding author.
E-mail address: rauleg@unam.mx (R. Escamilla).

http://dx.doi.org/10.1016/j.molstruc.2016.07.004
0022-2860/

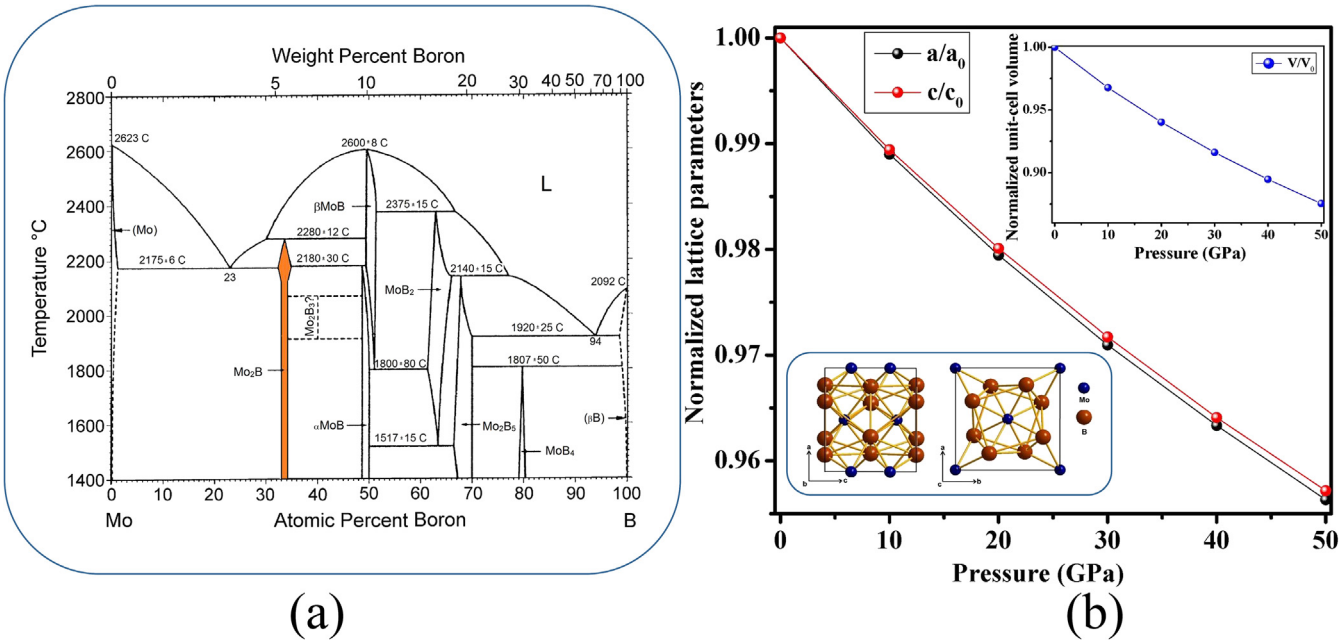

Fig. 1. (a) Mo–B phase diagram and (b) normalized lattice parameters: a/a_0 and c/c_0 as a function of pressure. The lower left inset in Fig. 1(b) shows the crystal structure of the Mo_2B phase with the *I*4/*m* space group viewed along the b axis (left) and along the c axis (right). The top right inset in Fig. 1(b) shows the normalized unit cell volume: V/V_0 as a function of pressure.

the metallic behavior [10–13]. However, the presence or absence of superconductivity in these phases has not been clarified to date. Another interesting aspect is related to the phase stability, which has generated much discussion in recent years [10,14,15]. M. Frotscher et al. showed through powder X-ray and neutron diffraction studies and by electron microprobe analysis that the Mo_2B_5 phase is unstable at atmospheric pressure [16]. However, P. Liu et al. showed using powder X-ray diffraction that the rhombohedral structure in Mo_2B_5 is stable up to 24.1 GPa and that their compressibility on the a-axis and c-axis is anisotropic [17]. Another example is the Mo_2B phase. Recently, D. Zhou et al. [11] studied the structural, elastic, vibrational and electronic properties of this phase using ab initio phonon calculations. They found a dynamically unstable structure when the *I*4/*mcm* space group is proposed, in contrast to what occurs when the *I*4/*m* space group is used.

In the following, we explore and compare with other studies the phase stability under high pressure for Mo_2B with the *I*/4*m* space group. We employ first-principles calculations based on the generalized gradient approximation (GGA). The motivation is that the application of high pressure allows for theoretical investigations of the phase stability and phase transitions due to changes in the lattice parameters of the crystal lattice. Until now, few studies have been conducted on molybdenum borides under high pressure [11,16,18–20]. Furthermore, in this work, we systematically investigate the mechanical, thermodynamic, vibrational and electronic properties of the *I*4/*m* space group, which have not previously been explored.

2. Calculation details

The first-principles calculations were performed using the CASTEP code [21,22] within the density functional theory (DFT) scheme [23,24]. The correlation functionals were treated by the generalized gradient approximation (GGA), as proposed by Perdew-Wang (PW91) [25]. The tightly bound core electrons were represented by Vanderbilt-type nonlocal ultra-soft pseudo-potentials [26]. During searching of the minimum energy configuration for a modeled system, the CASTEP code allows the Kohn-Sham equations to be solved using a plane wave basis. The former is connected to one of two parameters that affect the accuracy of the calculations: the cut-off kinetic energy; the second parameter is the number of k-points used to sample the Brillouin zone (BZ). The results converged when a 500 eV cut-off kinetic energy and 11 × 11 × 11 k-point mesh were used [27]. Careful convergence tests show that convergence of the total energy calculations is guaranteed with these parameters. The convergence tolerances were set as follows: 0.002 eV/Å for the maximum force on atoms, 10^{-4} Å for the maximum atomic displacement, and 0.003 GPa for the highest strain amplitude. The elastic coefficients were determined from first-principles calculations by applying a set of given homogeneous deformations with a finite value (maximum strain amplitude of 0.003 GPa) and calculating the resulting stress with respect to optimizing the internal degrees of freedom. Although the CASTEP code is designed for studying periodic systems, the selected convergence criteria define how computationally expensive each calculation becomes; however, the code provides two alternatives to calculate the vibrational properties of the modeled systems: by using the finite displacement or the linear response approximations. In this work, the first-principles investigations of the phonon dispersion relations and phonon modes are performed using the finite displacement method [28]. Moreover, some phonon-related thermodynamic properties, such as the internal energy (ΔE), the Helmholtz free energy (ΔF), the entropy (S) and the lattice contribution to the heat capacity C_v, were calculated in a quasi-harmonic approximation [29]. Finally, the Mulliken populations and atomic bonds were investigated by the projection of plane-wave states into a linear combination of atomic orbitals.

3. Results and discussion

3.1. Structural properties under pressure

Dimolybdenum boride Mo_2B (Al_2 Cu-type structure) shows a body-centered tetragonal structure (space group *I*4/*mcm*; point

group D_{4h} (4/*mmm*)), in which each unit cell contains 12 atoms: eight Mo atoms and four B atoms. The Wyckoff positions of the atoms in Mo_2B are Mo: 8 h (0.17, 0.67, 0) and B: 4 a (0, 0, 0.25). Each B atom has eight nearest Mo atoms. The coordination number of the Mo atom is 4, with four Mo–B bonds [1]. However, it has recently been reported that the Mo_2B structure with the *I*4/*mcm* space group is dynamically unstable at ambient pressure with respect to the *I*4/*m* space group [11]. For the *I*4/*m* space group, the Wyckoff positions are Mo: 8 h (0.1626, 0.6770, 0.0000) and B: 4 e (0.0000, 0.0000, 0.2871); see inset Fig. 1 (b) [30].

The Mo_2B structure with the *I*4/*m* space group was optimized for each pressure value up to 50.0 GPa with respect to internal parameters, energy, force, stress, and displacement. The optimized lattice parameters and unit cell volumes under pressure within the GGA-PW91 approximation are shown in Table 1. The overestimation of structural parameters is intrinsic with the GGA-PW91 approximation.

Comparing the optimized lattice parameters in Table 1 at ambient pressure (0.0 GPa) with those measured experimentally [30], we obtained errors of 0.16% and 0.25% for the lattice parameters *a* and *c*, respectively. In contrast, using the optimized lattice parameters with the *I*4/*mcm* group space reported in Ref. [12] and the experimental data [1], we obtained errors of 0.04% and 0.42% for lattice parameters *a* and *c*, respectively. It is observed that when using the *I*4/*mcm* space group, the optimized lattice parameters *a* and *c* are not very accurate because the error in lattice parameter *a* is considerably higher than that obtained in lattice parameter *c*. However, when using the *I*/4*m* space group, the optimized lattice parameters are consistent with those measured experimentally because the errors in both lattice parameters are similar. Therefore, we can assume that our calculations are more accurate when using the *I*/4*m* space group than when using the *I*4/*mcm* space group.

Fig. 1(b) shows the pressure dependence of the normalized lattice parameters a/a_0, c/c_0, and in the top right inset, the normalized unit cell volume V/V_0 (where a_0, c_0, and V_0 are the zero-pressure equilibrium structural parameters) is shown. As shown in Fig. 1 (b), the values of the structural parameters decrease almost linearly with increasing pressure. From the pressure derivatives of the normalized a/a_0 and c/c_0 lattice parameters, we determined the bulk linear compressibility perpendicular, $\beta_\perp = -\mathrm{dln}(a/a_0)/\mathrm{dP}$ and parallel, $\beta_\parallel = -\mathrm{dln}(c/c_0)/\mathrm{dP}$, to the *c* axis. The obtained $\beta_\perp$ and $\beta_\parallel$ values are -8.6808×10^{-4} GPa^{-1} and -8.5284×10^{-4} GPa^{-1}, respectively. These values indicate that the compressibility is isotropic because the bulk linear compressibility in both axes is similar $\beta_\perp/\beta_\parallel = 1.02$

Table 1
Optimized lattice parameters and unit cell volume of the Mo_2B intermetallic under pressure.

Pressure (GPa)	*a* (Å)	*c* (Å)	*V* (Å^3)
0.0	5.5617	4.7565	147.13
10.0	5.5051	4.7062	142.39
20.0	5.4474	4.6618	138.34
30.0	5.4002	4.6220	134.79
40.0	5.3578	4.5857	131.64
50.0	5.3188	4.5528	128.80
[a]Exp.	5.543	4.735	145.50
[b]GGA-PBE	5.5449	4.7550	146.20
[c]Exp.	5.5527	4.7443	146.29
[d]GGA-PW91	5.545	4.755	146.20

[a] Ref. [1].
[b] Ref. [14].
[c] Ref. [30].
[d] Ref. [12].

3.2. Elastic and mechanical properties under pressure

Table 2 shows the calculated values of the elastic constants, C_{11}, C_{12}, C_{13}, C_{33}, C_{44} and C_{66}, for the tetragonal Mo_2B structure. Fig. 2(a) shows the behavior of these elastic constants with pressure. The elastic constants are positive and satisfy the well-known Born criteria for tetragonal crystals, indicating that the structure of Mo_2B with space group *I*4/*m* is elastically stable up to P = 50.0 GPa, as shown in Fig. 2 (a). Mo_2B is generally prepared as a polycrystalline material; therefore, it is useful to estimate the corresponding mechanical parameters for this material. The theoretical polycrystalline elastic moduli for Mo_2B were calculated from the set of elastic constants. Hill [31] showed that the Voigt and Reuss equations represent the lower and upper limits of the polycrystalline constants. In this framework, the polycrystalline moduli are the arithmetic mean values of the moduli in the Voigt (B_V, G_V) and Reuss (B_R, G_R) approximations, and then, they are given by $B_H \equiv B$ and $G_H \equiv G$. The expressions for the Voigt and Reuss moduli can be found elsewhere [32,33]. Young's modulus (*E*) and Poisson's ratio (ν) are evaluated from the calculated values of the moduli. The elastic constants and elastic modulus monotonically increase under pressure, as shown in Table 2. At P = 0.0 GPa, the bulk modulus (*B*) of the Mo_2B compound (286 GPa) is considerably lower compared with c-BN (376 GPa) [34], slightly lower than MoB_2 (295 GPa) [35] and higher than that of Mo metal (230 GPa). According to Chiodo et al. [36], a material is ultra-incompressible if it has a bulk modulus between 365 and 395 GPa. Our results show that the material studied in this work and that reported by D. Zhou (B = 303 GPa) [11] are not ultra-incompressible. On the other hand, under pressure variations, the bulk modulus of Mo_2B increased from 286 to 474 GPa. From the common physical equation of the bulk modulus ($B = \Delta P/\Delta V$), one can expect an increase in B because of its direct relation to applied pressure.

According to the Pugh criteria [37], materials with a G/B value < 0.5 may behave as ductile materials; otherwise, the materials should be brittle. Our results show that the G/B ratio changes from 0.51 (P = 0.0 GPa) to 0.42 (P = 50.0 GPa). These values indicate a transition from brittle to ductile nature under pressure (see Fig. 2 (b)). The relative directionality of the bonding in the material also has an important effect on its hardness and can be determined from the G/B ratio. The Mo_2B at 0.0 GPa has the largest G/B ratio, which suggests the strongest directional bonding between Mo and B atoms, and this bonding decreases as the pressure increases.

The calculated Poisson ratio (ν) is an additional argument for the variation in the brittle/ductile behavior. For brittle materials, these values are small, whereas for ductile metallic materials, ν is typically 0.33. In our case, ν changes from 0.28 to 0.32; therefore, the behavior of Mo_2B tends from brittle to ductile.

The hardness (*H*) of a material always plays a significant role in applications. Using the evolutionary algorithm USPEX based on the formula of Knoop hardness (in GPa), hardness can be calculated as.

$$H = \frac{423.8}{V} n \left(\prod_{k=1}^{n} N_k X_k e^{-2.7 f_k} \right)^{1/n} - 3.4, \quad (1)$$

where N_k is the number of bonds of type k in the unit cell and *V* is the unit cell volume. X_k is the electron-holding energy of the bond *k*, and f_k is the ionicity indicator, which are defined in Refs. [39,40].

Table 2 shows the estimated theoretical hardness (*H*) as a function of pressure. Our predicted *H* value at 0.0 GPa is 19.3 GPa; this is slightly lower than the experimental value reported for Mo_2B (24.5 GPa) [9] and considerably lower than that for brittle materials such as c-BN (47 GPa) and diamond (85 GPa) [35].

Furthermore, these mechanical properties are slightly different

Table 2
Elastic constants (C_{ij}), bulk modulus (B), shear modulus (G), (G/B) ratio, Young's modulus (E), Poisson's ratio (ν) and hardness (H) of the Mo_2B intermetallic under pressure. All units are in GPa.

Pressure	C_{11}	C_{12}	C_{13}	C_{33}	C_{44}	C_{66}	B	G	G/B	E	ν	H
0.0	475	183	200	455	147	163	286	146	0.51	373	0.28	19.3
10.0	544	198	228	531	152	169	325	159	0.49	410	0.29	20.1
20.0	598	231	260	584	163	190	365	171	0.47	444	0.30	20.8
30.0	639	255	301	601	173	201	399	177	0.44	462	0.31	21.7
40.0	695	280	331	647	180	213	436	186	0.43	489	0.31	24.4
50.0	749	307	365	694	195	229	474	200	0.42	525	0.32	25.3
[a]GGA-PBE	518	180	208	496	155	161	303	156	0.51	399	0.28	21.2
[b]GGA-PBE	498	191	210	465	153	165	298	150	0.50	387	0.28	–
[c]Exp.												24.5
[c]GGA-PBE	500	202	–	515	152	151	301	151	0.50	389	0.28	18.9
[d]GGA-PBE	489	168	208	455	150	164	279	140	0.50	361	0.29	13.3

[a] Ref. [11] with space group *I*4/*m*.
[b] Ref. [14] with space group *I*4/*mcm*.
[c] Ref. [9] with space group *I*4/*mcm*.
[d] Ref. [38] with space group *I*4/*mcm*. The values were taken at P = 0.0 GPa.

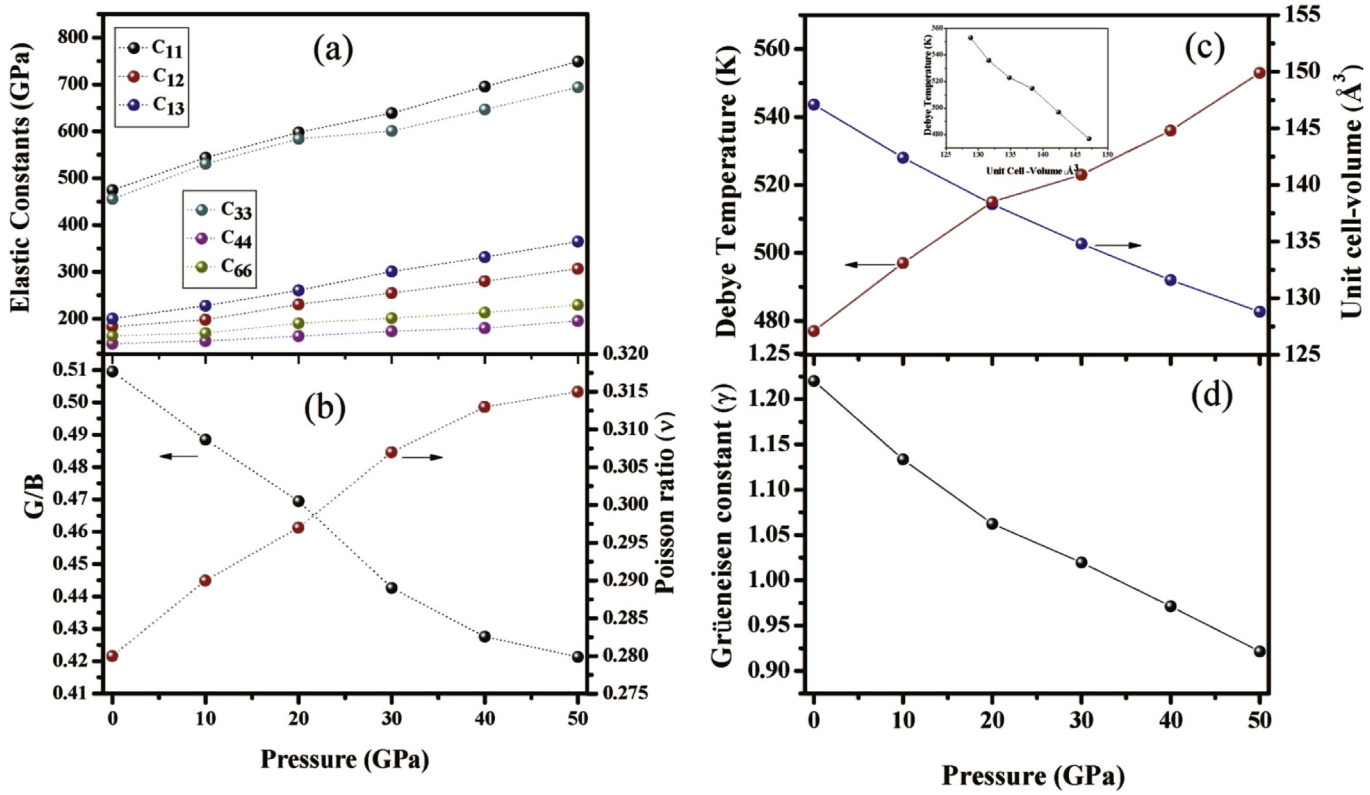

Fig. 2. (a) Elastic constants, (b) variation of the G/B – Poisson ratio (ν), (c) Debye temperature θ_D – unit cell volume and (d) Grüneisen parameter (γ) of the Mo_2B intermetallic under pressure. The inset in (c) shows the Debye temperature as a function of the unit cell.

from those reported for the space group *I*4/*mcm*, as compared at the bottom of Table 2.

Other important physical quantities that can be deduced from the obtained bulk modulus (B) and shear modulus (G) are the Debye temperature (θ_D) and the sound velocity [41], and the formula is as follows:

$$\theta_D = \frac{\hbar}{k_B}\left[\frac{6\pi^2 N}{V}\right]^{1/3} v_m, \tag{2}$$

where $\hbar$ is Plank's constant, k_B is Boltzmann's constant, N is the number of atoms in the unit cell, and v_m is the average sound velocity. The v_m depends on v_l and v_t, the longitudinal and transverse elastic wave velocities, respectively, as:

$$v_m = \left[\frac{1}{3}\left(\frac{2}{v_t^3}+\frac{1}{v_l^3}\right)\right]^{-1/3}, \tag{3}$$

and v_l and v_t are determined as

$$v_l = \sqrt{\frac{3B+4G}{3\rho}}; v_t = \sqrt{\frac{G}{\rho}}, \tag{4}$$

As shown in Table 3, the Debye temperature increases under

Table 3
Debye temperature (θ_D) and Grüneisen constant (γ) of the Mo_2B intermetallic under pressure.

Pressure (GPa)	θ_D (K)	γ
0.0	477	1.22
10.0	497	1.13
20.0	515	1.06
30.0	523	1.02
40.0	536	0.97
50.0	553	0.92
[a]Calc.	494	
[b]Calc.	56[a]	

[a] Ref. [11] The value was calculated with space group *I*4/*m*.
[b] Ref. [38] with space group *I*4/*mcm*. The values were taken at P = 0.0 GPa.

Table 4
IR modes and Raman modes of the Mo_2B intermetallic under pressure.

Pressure (GPa)	IR modes (cm^{-1})	Raman modes (cm^{-1})
0.0	207.6 E_u	163.4 A_g
	398.6 A_u	221.6 B_g
	542.1 E_u	216.7 E_g
		224.0 B_g
		225.5 A_g
		449.8 A_g
		532.9 E_g
50.0	266.6 E_u	205.3 A_g
	496.1 A_u	277.1 B_g
	650.5 E_u	295.5 E_g
		306.6 B_g
		295.6 A_g
		571.6 A_g
		665.4 E_g

compression due to stiffening of the lattice. Therefore, the corresponding phonon frequencies will also be modified. This effect can be quantified by the Grüneisen constant γ [42], which is defined as follows:

$$\gamma = -\frac{V\mathrm{d}\theta_D}{\theta_D \mathrm{d}V} \quad (5)$$

where V is the unit cell volume.

Fig. 2 (c) shows a linear increase in θ_D as a function of pressure, with a pressure coefficient of 1.44 K/GPa. The inset in Fig. 2 (c) shows θ_D as a function of unit cell volume, and the volume coefficient of the Debye temperature estimated from the linear approximation is -3.96 K/Å^3. Moreover, the calculated values of the Grüneisen constant as a function of pressure are plotted in Fig. 2 (d). At 0.0 GPa, $\gamma = 1.22$; with increasing pressure, γ linearly decreases due to the weakened dependence of the vibrational frequencies on pressure.

3.3. Vibrational properties and phonon dispersion curves under pressure

Fig. 3(a) shows the obtained phonon dispersion curves along the high-symmetry directions, and Fig. 3(b) presents the corresponding partial density of phonon states for 0.0 GPa and 50.0 GPa. No imaginary phonon frequency is observed in the entire BZ, indicating that the phase is stable under pressure.

The primitive cell of the tetragonal structure, with space group *I*4/*m*, contains four formula units. The theoretical group analysis of the eigenmodes of the tetragonal structure (C_{4h}) yields $A_u + 2^1 E_u + 2^2 E_u$ IR-active modes (acoustic modes not included) and $3A_g + 2B_g + 2^1 E_g + 2^2 E_g$ Raman-active modes, as listed in Table 4.

The partial density of phonon states of Mo_2B at zero GPa can be divided into two regions, as clearly shown in Fig. 3(b). The first region is localized at low frequency and belongs to the acoustic phonon modes. In this region, the position of the maximum peak appears below 250 cm^{-1}, and it is associated with the molybdenum atoms. The optical phonon modes are located at high frequency.

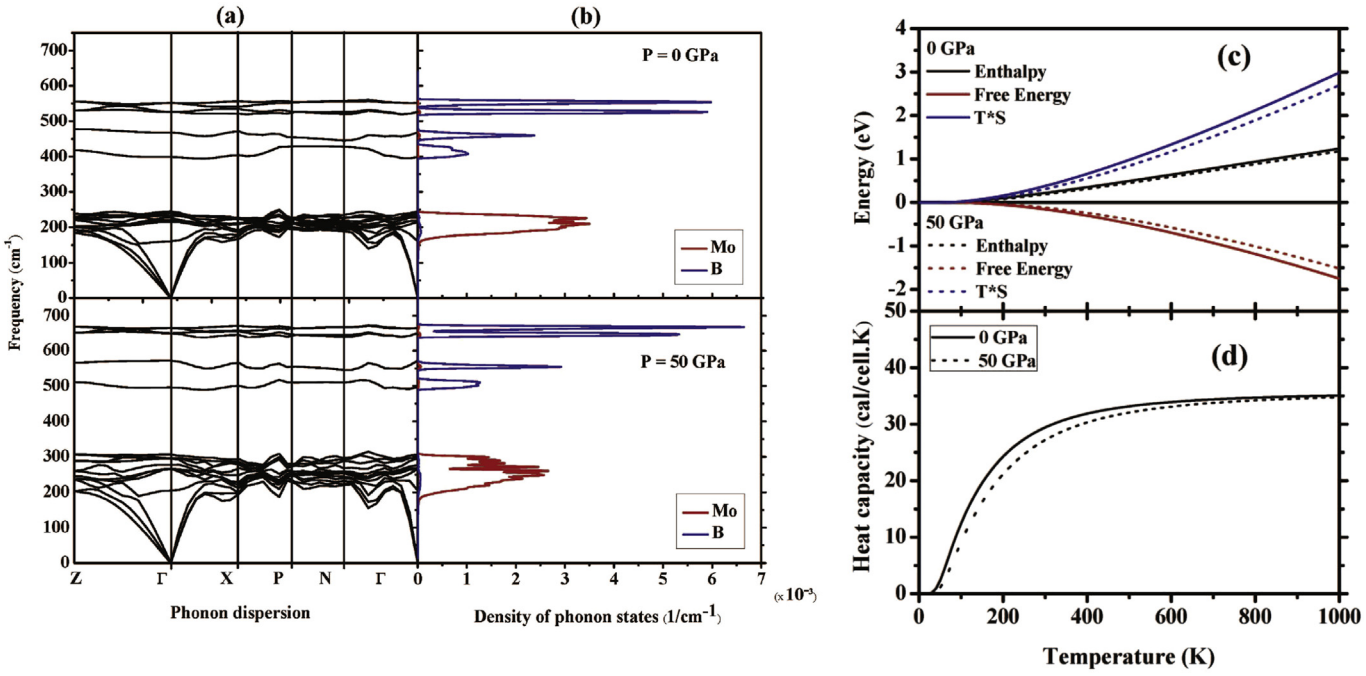

Fig. 3. (a) Calculated phonon dispersion curves; (b) partial phonon density of states; (c) temperature dependence of enthalpy, free energy, and T*S; and (d) heat capacity dependence of temperature for Mo_2B at P = 0.0 GPa and 50.0 GPa.

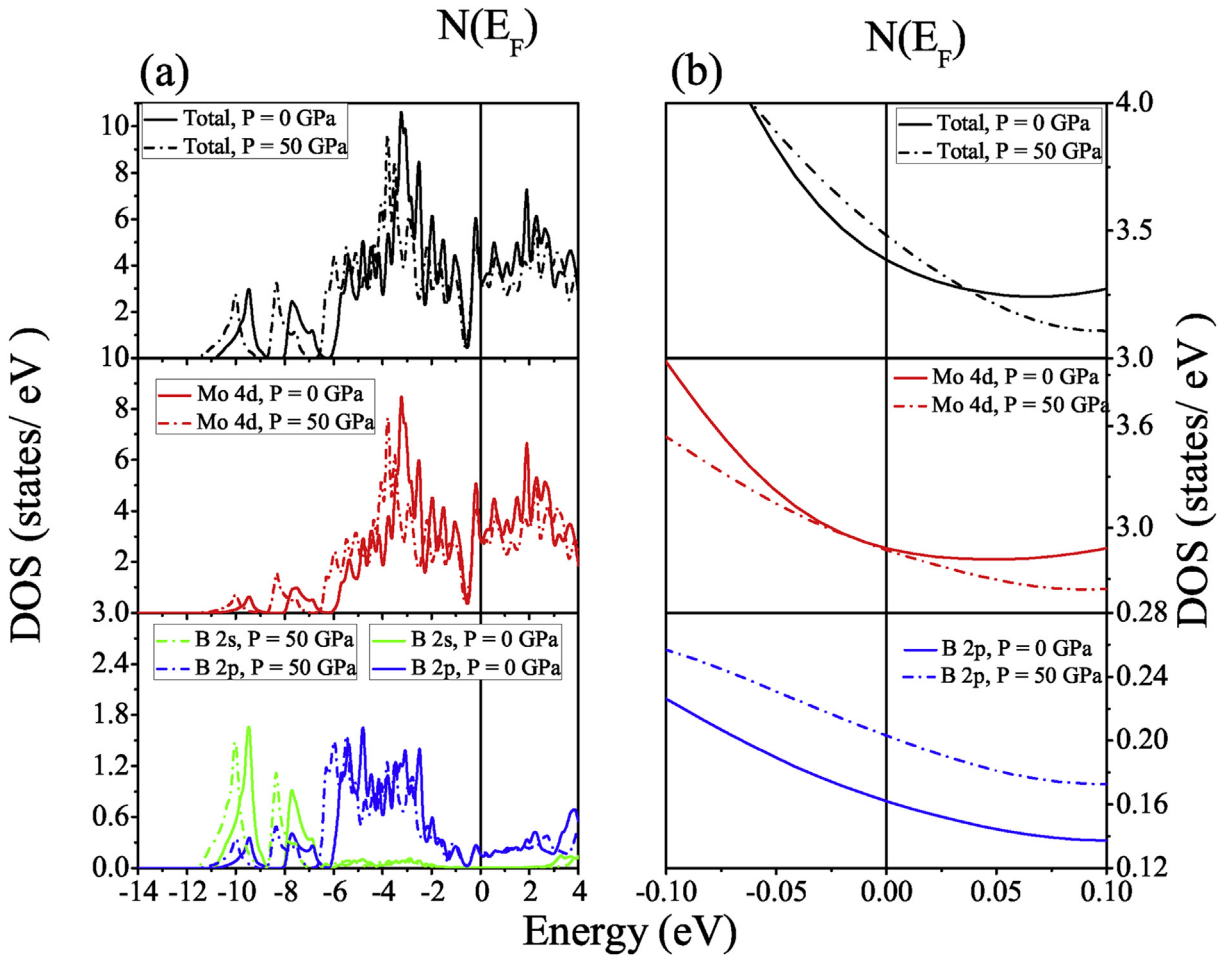

Fig. 4. (a) Total and partial electronic densities of states of the Mo_2B intermetallic at P = 0.0 (solid line) and 50.0 GPa (dots), (b) Zoom from −0.1 to 0.1 eV of the total and partial electronic densities of states.

Two maximum peaks are localized in this region, at approximately 427 cm^{-1} and 540 cm^{-1}, respectively. The first one is from both Mo and B, and the second is from boron atoms. This result is expected because the boron atoms are lighter than the molybdenum atoms, resulting in comparatively weaker electron-phonon interactions; however, Escamilla et al. [43] showed that in the Mo_2B with space group *I*4/*m*, the electron-phonon interaction is intermediate.

Table 5
Mulliken population analysis results of the Mo_2B intermetallic under pressure.

Pressure (GPa)		s	p	d	Total electrons	Charge states
0.0	B	1.03	2.45	0	3.48	−0.48
	Mo	2.16	6.65	4.95	13.76	0.24
10.0	B	1.03	2.47	0	3.50	−0.50
	Mo	2.15	6.64	4.96	13.75	0.25
20.0	B	1.02	2.49	0	3.51	−0.51
	Mo	2.13	6.64	4.98	13.75	0.25
30.0	B	1.02	2.50	0	3.52	−0.52
	Mo	2.12	6.63	4.99	13.74	0.26
40.0	B	1.02	2.52	0	3.53	−0.53
	Mo	2.11	6.62	5.01	13.73	0.27
50.0	B	1.01	2.53	0	3.54	−0.54
	Mo	2.10	6.61	5.02	13.73	0.27
[a]GGA-PBE	B	1.03	2.41	0	3.45	−0.45
	Mo	2.15	6.67	4.95	13.78	0.22

[a] Ref. [13].

Fig. 3(b) shows a gap in the region between low frequency and high frequency. This gap is formed because the mass differences between the molybdenum and boron atoms strongly affects the maximum and minimum values of the acoustic and optical branches. The acoustic and optical branches are separated by a frequency gap from 148 to 179 cm^{-1} for 0.0–50.0 GPa. Consequently, with increasing pressure, a shift is induced in the branches toward high frequency. Similar results for the increase in the gap and shift in the branches under pressure in borides have been reported by other author [15,44,45].

3.4. Thermodynamic properties under pressure

Fig. 3 (c) shows the enthalpy, entropy and free energy under pressure. The Helmholtz free energy, F = E − TS, is the relevant potential in an ensemble, where the volume and temperature are independent variables. As shown in Fig. 3(c), below 100 K, the values of the enthalpy, entropy, and free energy are almost zero. Above 100 K, the free energy at 0.0 GPa decreases faster with increasing temperature with respect to 50.0 GPa, and the entropy multiplied by the temperature at 0.0 GPa increases rapidly as the temperature increases with respect to 50.0 GPa, resulting in a linearly increasing relationship between the variations of enthalpy.

Fig. 3(d) shows the variations of the lattice heat capacity with temperature. We observed that the heat capacity C_v increases with the applied temperature but decreases under pressure. Below a

temperature of approximately 800 K, C_v increases very rapidly with the temperature; above 800 K, C_v increases slowly and gradually approaches the Dulong-Petit limit.

3.5. Electronic properties under pressure

Fig. 4 (a) presents the total and partial electronic densities of states of Mo_2B at 0.0 and 50.0 GPa. The calculated equilibrium total density of states at the Fermi level E_F is 3.42 states/eV; this value is consistent with the results of Ref. [11].

The contributions of the B 2s and B 2p states at 0.0 GPa are comprised between −6.0 and −11.0 eV and −6.0 to −1.0 eV, respectively. Close to the Fermi level, the calculated DOS is predominated by the Mo 4*d* states; therefore, metallic-like Mo–Mo bonding occurs due to the overlap of the Mo 4*d* states at the Fermi level. The feature from −6.0 and −1.0 eV is due to covalent hybridization between the Mo 4*d* - B 2p bonding states.

Compared to the DOS at 0.0 GPa with respect to 50.0 GPa, the total and partial DOS move toward lower energies. At 50.0 GPa, the peak and height of the DOS become lower. According to our calculations, an increase in the pressure leads to an increase in $N(E_F)$ due to the increase in $N_B(E_F)$ associated with the boron states; the $N_{Mo}(E_F)$ associated with the molybdenum states remain virtually unchanged, as shown in Fig. 4(b). These results show that the main contribution to $N(E_F)$ is due to boron.

To understand the changes in the $N(E_F)$, we calculated the charge transfer between B and Mo atoms using Mulliken atomic population analysis (see Table 5). Our results indicate that B carries the negative charges and that Mo carries the positive charges from 0.0 to 50.0 GPa. These values change from −0.48 to −0.54 electrons for the B atoms and from 0.24 to 0.27 for the Mo atoms. Therefore, one can suggest an electron transfer mechanism between the B and Mo atoms, for example, to p-d hybridized covalent bonding between B and Mo. In this case, extra electrons are transferred from Mo to B.

4. Conclusions

In this paper, the structural, elastic, vibrational, thermodynamic and electronic properties of the Mo_2B intermetallic under pressure were studied using first-principles calculations within the generalized gradient approximation (GGA). We determined that the effect of pressure on the crystal structure is reflected in a contraction of the unit cell volume. The similar reduction in the lattice parameters with pressure indicates an isotropic compressibility in the structure with space group *I*4/*m*. Consequently, the elastic constants, elastic modulus, and hardness monotonically increase. The mechanical properties also show that the behavior of Mo_2B tends from brittle to ductile with pressure. It is found that the Debye temperature (θ_D), calculated using the elastic constant, is increased under pressure. On the other hand, the phonon dispersion curves showed no imaginary phonon frequency in the entire BZ under pressure, indicating a dynamically stable *I*4/*m* space group. Two pronounced regions are observed, which are related to the acoustic part at low frequency around 250 cm^{-1} associated with Mo atoms and the optical part at high frequency around 540 cm^{-1} associated with B atoms of the phonon spectrum. A shift to high-frequency values is observed under pressure. The thermodynamic properties enthalpy, entropy, free energy and heat capacity are reported and discussed. Finally, according to our calculations, an increase in the pressure would lead to an increase in the $N(E_F)$ of Mo_2B, mainly due to the increase in the contribution of B 2p states at the Fermi level. Moreover, the electron transfer is increased from Mo to B atoms as a function of pressure.

Acknowledgements

The authors thank the projects DGAPA-UNAM IN104314, SIP-20141640 and SIP-20141641 from IPN. Financial support to PASPA- DGAPA (2014-2015); also, for their technical help to F. Silvar, M.M.S. Alberto Lopez-Vivas, J. Morales and C. González. Calculations were performed using resources from the Supercomputing Center DGTIC-UNAM.

References

[1] R. Kiessling, A. Wetterholm, L.G. Sillén, A. Linnasalmi, P. Laukkanen, The crystal structures of molybdenum and tungsten borides, Acta Chem. Scand. 1 (1947) 893–916.
[2] R. Steinitz, I. Binder, D. Moskowite, System molybdenum-boron and some properties of the molybdenum-borides, J. Met. 4 (1952) 983–987.
[3] K. Kudaka, K. Izumi, T. Sasaki, S. Okada, Mechanochemical synthesis of MoB_2 and Mo_2B_5, J. Alloys Compd. 315 (2001) 104–107.
[4] F. Galasso, J. Pinto, The metal borides in boron fiber cores; identification of MoB_4, Trans. Inst. Min. Metall. Sect. A 242 (1968) 754–758.
[5] A.W. Weimer, Carbide, Nitride, and Boride Materials Synthesis and Processing, Chapman and Hall, 1997.
[6] E.M. Savitskii, V.V. Baron, Y.V. Efimov, M.I. Bychkova, L.F. Myzenkova, Superconducting Materials, Plenum Press, 1973.
[7] J.J. Engelhardt, Superconducting isotope effect in molybdenum boride and tungsten boride, Phys. Rev. 179 (1969) 452–458.
[8] K.E. Spear, P.K. Liao, The B - Mo (boron-molybdenum) system, Bull. Alloy Phase Diagrams. 9 (1988) 457–466.
[9] M. Zhang, H. Wang, H. Wang, T. Cui, Y. Ma, Structural modifications and mechanical properties of molybdenum borides from first principles, J. Phys. Chem. C 114 (2010) 6722–6725.
[10] I.R. Shein, K.I. Shein, A.L. Ivanovskii, First-principles study on the structural, cohesive and electronic properties of rhombohedral Mo_2B_5 as compared with hexagonal MoB_2, Phys. B Condens. Matter. 387 (1–2) (2007) 184–189.
[11] D. Zhou, J. Wang, Q. Cui, Q. Li, Crystal structure and physical properties of Mo_2B: first-principle calculations, J. Appl. Phys. 115 (2014) 113504–113508.
[12] H. Si Abdelkader, H.I. Faraoun, Ab initio investigation of Al/Mo_2B interfacial adhesion, Comput. Mater. Sci. 50 (2011) 880–885.
[13] C.T. Zhou, J.D. Xing, B. Xiao, J. Feng, X.J. Xie, Y.H. Chen, First principles study on the structural properties and electronic structure of X_2B (X = Cr, Mn, Fe, Co, Ni, Mo and W) compounds, Comp. Mater Sci. 44 (2009) 1056–1064.
[14] S. Aryal, M.C. Gao, L. Ouyang, P. Rulis, W.Y. Ching, Ab initio studies of Mo-based alloys: mechanical, elastic, and vibrational properties, Intermetallics 38 (2013) 116–125.
[15] X. Chong, Y. Jiang, R. Zhou, J. Feng, Stability, chemical bonding behavior, elastic properties and lattice thermal conductivity of molybdenum and tungsten borides under hydrostatic pressure, Ceram. Int. 42 (2016) 2117–2132.
[16] M. Frotscher, W. Klein, J. Bauer, C.M. Fang, J.F. Halet, A. Senyshyn, C. Baehtz, B. Albert, M_2B_5 or M_2B_4 a reinvestigation of the Mo/B and W/B system, Z. Anorg. Allg. Chem. 633 (2007) 2626–2630.
[17] P. Liu, F. Peng, S. Yin, F. Liu, Q. Wang, X. Zhu, P. Wang, J. Liu, D. He, Exploring the behavior of molybdenum diboride $(MoB)_2$: a high pressure x-ray diffraction study, J. Appl. Phys. 115 (2014) 163502–163505.
[18] L. Xiong, J. Liu, X. Zhang, Q. Tao, P. Zhu, Radial X-ray diffraction study of the static strength and equation of state of MoB_2 to 85 GPa, J. Alloys Compd. 623 (2015) 442–446.
[19] M. Zhang, H. Yan, Q. Wei, H. Wang, Pressure-induced phase transition and mechanical properties of molybdenum diboride: first principles calculations, J. Appl. Phys. 112 (2012) 013522–013528.
[20] M. Sekar, N.V. Chandra Shekar, S. Appalakondaiah, G. Shwetha, G. Waitheeswaran, V. Kanchana, Structural stability of ultra-incompressible Mo_2B: a combined experimental and theoretical study, J. Alloy. Comp. 654 (2016) 554–560.
[21] M.C. Payne, M.P. Teter, D.C. Allan, T.A. Arias, J.D. Joannopoulos, Iterative minimization techniques for ab initio total-energy calculations: molecular dynamics and conjugate gradients, Rev. Mod. Phys. 64 (1992) 1045–1097.
[22] M.D. Segall, P.J. Lindan, M.J. Probert, J.C. Pickard, P.J. Hasnip, S.J. Clark, M.C. Payne, First-principles simulation:ideas, illustrations and the CASTEP code, J. Phys- Condens. Matter. 14 (2002) 2717–2744.
[23] P. Hohenberg, W. Kohn, Inhomogeneous electron gas, Phys. Rev. 136 (1964) B864–B871.
[24] W. Kohn, L.J. Sham, Self-consistent equations including exchange and correlation effects, Phys. Rev. 140 (1965) A1133–A1138.
[25] J.P. Perdew, Y. Wang, Accurate and simple analytic representation of the electron-gas correlation energy, Phys. Rev. B 45 (1992) 13244–13249.
[26] D. Vanderbilt, Soft self-consistent pseudopotentials in a generalized eigenvalue formalism, Phys. Rev. B 41 (1990) 7892–7895.
[27] H.J. Monkhorst, J.D. Pack, Special points for Brillouin-zone integrations, Phys. Rev. B 13 (1976) 5188–5192.
[28] E. Kaxiras, Atomic and Electronic Structure of Solids, Cambridge University Press, 2003.

[29] S. Baroni, S. de Gironcoli, A. Dal Corso, P. Giannozzi, Phonons and related crystal properties from density-functional perturbation theory, Rev. Mod. Phys. 73 (2001) 515–562.
[30] E.E. Havinga, H. Damsma, P. Hokkeling, Compounds and pseudo-binary alloys with the $CuAl_2(C)_{16}$-type structure I. preparation and X-ray results, J. Less Common Met. 27 (1972) 169–186.
[31] R. Hill, The elastic behavior of a crystalline aggregate, Proc. Phys. Soc. A 65 (1952) 349–354.
[32] W. Voigt, Lehrbuch der Kristallphysik, Teubner, Leipzig (, 1928.
[33] A. Reuss, Berechnung der Fliebgrenze von Mischkristallen auf grund der plastizitatsbedinggung fer einkristalle, Z. Angew. Math. Mech. 9 (1929) 49–58.
[34] R.F. Zhang, Z.J. Lin, Y.S. Zhao, S. Veprek, Superhard materials with low elastic moduli: three-dimensional covalent bonding as the origin of superhardness in B_6 O, Phys. Rev. B 83 (2011) 092101–092105.
[35] S. Yin, D. He, C. Xu, W. Wang, H. Wang, L. Li, L. Zhang, F. Liu, P. Liu, Z. Wang, C. Meng, W. Zhu, Hardness and elastic moduli of high pressure synthesized MoB_2 and WB_2 compacts, High Press. Res. An Int. J. 33 (2) (2013) 409–417.
[36] S. Chiodo, H.J. Gotsis, N. Russo, E. Sicilia, OsB_2 and RuB_2, ultra-incompressible, hard materials: first-principles electronic structure calculations, Chem. Phys. Lett. 425 (2006) 311–314.
[37] S.F. Pugh, XCII. Relations between the elastic moduli and the plastic properties of polycrystalline pure metals, Phil. Mag. 45 (1954) 823–843.
[38] B. Xiao, J. Feng, C.T. Zhou, J.D. Xing, X.J. Xie, Y.H. Cheng, R. Zhou, The elasticity, bond hardness and thermodynamic properties of X_2 B (X=Cr, Mn, Fe, Co, Ni, Mo, W) investigated by DFT theory, Phys. B 405 (2010) 1274–1278.
[39] K. Li, X. Wang, F. Zhang, D. Xue, Electronegativity identification of novel superhard materials, Phys. Rev. Lett. 100 (2008) 235504–235508.
[40] A.O. Lyakhov, A.R. Oganov, Evolutionary search for superhard materials: methodology and applications to forms of carbon and TiO_2, Phys. Rev. B 84 (2011) 092103–092106.
[41] L.O. Anderson, A simplified method for calculating the debye temperature from elastic constants, Phys. Chem. Solids. 24 (1963) 909–917.
[42] J.P. Poirier, Introduction to the Physics of the Earthś Interior, Cambridge University Press, 2000.
[43] R. Escamilla, E. Carvajal, M. Cruz-Irisson, F. Morales, L. Huerta, E. Verdin, XPS study of the electronic density of states in the superconducting Mo_2 B and Mo_2 BC compounds, J. Mater. Sci. 51 (2016) 6411–6418.
[44] I. Loa, K. Kunc, K. Syassen, MgB_2 and AlB_2 at high pressures, High Press. Res. 23 (1–2) (2003) 129–134.
[45] Z. Meiguang, Y. Haiyan, Q. Wei, W. Wang, Pressure-induced phase transition and mechanical properties of molybdenum diboride: first principles calculations, J. Appl. Phys. 112 (2012) 013522–013528.